Power Reversal Strategies for Hybrid LCC/MMC HVDC Systems

Gen Li, *Member, IEEE*, Ting An, Jun Liang, *Senior Member, IEEE*, Wei Liu, *Member, IEEE*, Tibin Joseph, *Member, IEEE*, Jingjing Lu, Marcio Szechtman, *Life Fellow, IEEE*, Bjarne R. Andersen, *Fellow, IEEE*, and Yuanliang Lan

***Abstract*—Power reversal control strategies for different types of hybrid line-commutated-converter (LCC)/modular multi-level converter (MMC) based high-voltage direct-current (HVDC) systems have been proposed with the consideration of system configurations and MMC's topologies. The studies show that the full-bridge (FB) MMC gives better performance than half-bridge (HB) MMCs in terms of power reversal in hybrid LCC/MMC systems. The modulation method employed in this paper can achieve a smooth online polarity reversal for hybrid LCC/FB-MMC HVDC systems. Additional DC switches and/or discharging resistors may be needed to reverse the DC polarity of LCC/HB-MMC HVDC systems. Based on the proposed strategies, the power reversal processes of the studied systems can be accomplished within several seconds. The speed can be changed according to system operation requirements. The effectiveness of the proposed control strategies has been verified through simulations conducted in PSCAD/EMTDC.**

***Index Terms*—FB-MMC, HB-MMC, hybrid LCC/MMC, LCC-HVDC, MMC-HVDC, power reversal.**

I. Introduction

HIGH-VOLTAGE direct-current (HVDC) transmission has been widely accepted as one of the most efficient technologies to transfer bulk power over long-distances [1]–[4]. Frequent power reversals may be needed in HVDC systems that interconnect two AC power grids [5], [6]. In line-commutated-converter (LCC) based HVDC systems, the power flow reversal is accomplished by changing the DC polarity of LCCs [7]. This demerit limits the application of LCC-HVDC technology in multi-terminal DC (MTDC) grids [8].

Manuscript received May 19, 2019; revised December 16, 2019; accepted January 1, 2020. Date of publication March 30, 2020; date of current version January 13, 2020. This work was supported by Science and Technology Project of the State Grid Corporation of China, "HVDC Systems/Grids for Transnational Interconnections", project number: SGTYHT/16-JS-198.

G. Li, J. Liang (corresponding author, e-mail: LiangJ1@cardiff.ac.uk), W. Liu and T. Joseph are with the School of Engineering, Cardiff University, Cardiff, CF24 3AA, U. K.

T. An and J. Lu are with the Global Energy Interconnection Research Institute, Beijing 102211, China.

M. Szechtman is with the Eletrobras Cepel, Rio de Janeiro, 26053-121 Brazil.

B. R. Anderen is with the Andersen Power Electronic Solutions, Bexhill-On-Sea, TN39 4QL U. K.

Y. Lan is with Global Energy Interconnection Research Institute Europe GmbH, Kantstr, 162 Berlin, Germany.

DOI: 10.17775/CSEEJPES.2019.01050

The voltage-source-converter (VSC) based HVDC technology, especially the modular multilevel converter (MMC) HVDC, shows many technical advantages compared to LCC-HVDC. One of MMCs' advantages compared to its LCC counterpart is that it has the same voltage polarity under bidirectional power flows [9]. This advantage makes MMC based technologies suitable for MTDC applications [10]. However, MMC HVDC still faces some challenges, such as its high capital cost, power losses and system complexities [2].

Hybrid LCC/MMC HVDC has been considered as a possible and effective alternative to combine the merits of the two technologies in terms of power losses, capital costs and flexible operations [11]–[14]. Hybrid LCC/MMC HVDC schemes were studied in literature to analyze their technical feasibility, operational and control strategies. References [5], [6] describe system configurations and control of the Skagerrak hybrid LCC/MMC HVDC project wherein the MMC and LCC links operate as the positive and negative poles to form a bipolar system. References [15], [16] study the operation and control of another topology of hybrid LCC/MMC HVDC link in which the LCC and MMC operate as a rectifier and an inverter, or vice versa. The start-up and shut-down strategies for hybrid LCC/MMC MTDC grids have been proposed in [17]. Reference [18] develops the valve-bridge bypassing strategies for hybrid LCC/MMC ultra HVDC systems. The control and protection of hybrid LCC/MMC MTDC networks underDC faults have been investigated in [9] and [19]. The aforementioned literature primarily focused on the operation, control and protection of hybrid LCC/MMC HVDC systems. However, few studies focus on the power reversal of hybrid LCC/MMC HVDC systems.

Methods and arrangement to reverse the power flow of LCC-HVDC links have been proposed in [20], [21]. However, the control strategy cannot be directly applied in hybrid LCC/MMC HVDC systems due to the different characteristics between the LCC and the MMC. Power reversal strategies have been proposed in [7] and [22] for LCC/half-bridge (HB) MMC and LCC/full-bridge (FB) MMC links in which the LCC and the MMC operate as the two terminals in the links. The proposed power reversal strategy for the LCC/HB-MMC system in [7] involves additional DC line discharging switches and resistors which increases capital costs. More importantly, the complexity and time of the power reversal process have been increased. The power reversal strategy proposed in [22] reverses the DC polarity of the FB-MMC by directly reversing

2096-0042 © 2019 CSEE

the output voltage of its submodules (SMs). This method may induce large transient overcurrents as the polarity reversed FB-MMC is still connected with the DC line, whose polarity has not yet changed.

The power reversal strategies for LCC/HB-MMC links wherein the HB-MMC and LCC links serve as the positive and negative poles are investigated in [5] and [6]. However, only the power reversal process of the HB-MMC link in the system is introduced. The coordination with the LCC link is not provided. Moreover, the proposed strategies in [5] and [6] are not verified through simulation results. In addition, the strategies for LCC/FB-MMC links wherein the FB-MMC and LCC links serve as the positive and negative poles are not investigated in the open literature. Furthermore, in some cases, a rapid or emergency online power reversal, from export to import, may be required to support the HVDC grid interconnected AC systems. For instance, to modulate their power automatically in response to AC system frequency variations or to provide synthetic inertia to support AC systems. Therefore, the power reversal strategy for hybrid LCC/MMC MTDC grids needs to be investigated.

In this paper, the power reversal strategies for different types of hybrid LCC/MMC systems are investigated by taking the system configurations and MMC's topologies into consideration. Control strategies are proposed to achieve a fast and reliable power reversal. The proposed strategies are verified in simulations conducted in PSCAD/EMTDC.

II. Hybrid HVDC Links with Mixed Poles

An MMC-HVDC link can be installed in parallel with an LCC-HVDC link to form a bipolar hybrid LCC/MMC HVDC system, such as the Skagerrak interconnection project [5], [6]. Fig. 1 shows a bipolar hybrid HVDC link wherein one pole is an MMC-HVDC and the other is an LCC-HVDC. The power flow between the two poles is balanced during normal operations and there will be minor unbalanced current in the dedicated metallic return. In this system, each pole can operate in the monopolar mode through the metallic return in case of failures or scheduled maintenance in one pole [8].

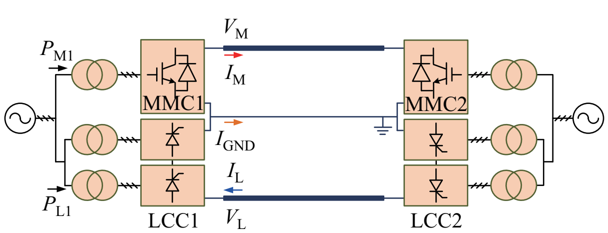

Fig. 1. A hybrid HVDC with mixed LCC and MMC links.

As the LCC operates as a current source, the DC current in the LCC always remains in one direction. Power reversal in the LCC link can be achieved by reversing the LCCs' DC polarity through changing their control modes [21]. At the same time, to coordinate with the LCC link, the DC polarity of the MMC link also needs to be changed during the power reversal process. However, the control strategies will be different when different types of MMCs are deployed in the MMC-based link.

It is known that the HB-MMC is not able to produce a negative DC voltage. Therefore, additional devices are needed in the DC terminal of the HB-MMC to accomplish the polarity reversal. Differing from the HB-MMC, the FB-MMC has the capability of changing its DC polarity thanks to its SM's configuration. Therefore, a fast online polarity reversal can be achieved in FB-MMC HVDC links.

To get a better understanding of operational performance, the power reversal strategies for both HB-MMC and FB-MMC based bipolar hybrid HVDC links are investigated in the next sections.

A. Mixed LCC and HB-MMC Links

Assume that the MMCs shown in Fig. 1 are HB-MMCs. Both of them will be equipped with four high-speed switches (S_{P1}, S_{P2}, S_{N1}, S_{N2}) on their DC terminals to change the polarity so that the DC current always flows in the same direction independently of the power flow directions. As the HB-MMCs will be shut-down and re-started during the power reversal process, the AC grid main breaker (BRK_{AC}) and the breaker (BRK_R) used to bypass the start-up resistor will be employed. Fig. 2 shows the DC side switches and AC side breakers. Moreover, in one of the HB-MMCs, a high-speed switch (S_D) and a discharging resistor (R) are installed in its DC terminal to discharge the DC line during the polarity reversal process. The initial status of the DC side switches and AC side breakers before starting the power reversal is given in Table I.

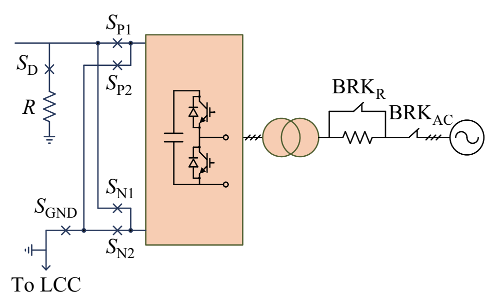

Fig. 2. An HB-MMC equipped with DC side switches and AC side breakers.

TABLE I
Initial Status of the DC Switches and AC Breakers

Switches or Breakers	Initial Status
BRK_{AC}	Closed
BRK_R	Closed
S_{P1}, S_{N2}	Closed
S_{P2}, S_{N1}	Open
S_D	Open
S_{GND}	Closed

The power in the MMC link will be reduced to zero once a power reversal order is received from the higher level control system. Then the MMCs will be blocked. The AC side breakers BRK_{AC} and BRK_R will then open to disconnect the MMCs from their AC grids. When the AC side breakers are fully opened, the switches S_{P1}, S_{N2} and S_{GND} will open to disconnect the MMCs from the DC line and the neutral ground. At last, the switch S_{D} will be closed to discharge the DC line.

The switch S_{D} will open once the DC line's voltage is discharged to zero. After that, the switches S_{P2}, S_{N1} and S_{GND} will be closed to reconfigure the connection between the DC line and the MMC. Then the main breaker $\mathrm{BRK_{AC}}$ will be closed. The DC line will be charged through the uncontrollable bridge. The start-up resistor will limit the current during the charging process. The bypass breaker $\mathrm{BRK_{R}}$ will be closed when the DC voltage reaches to the valve-side AC line voltage. Then the MMCs will be deblocked. To mitigate transient overcurrent and overvoltage, the power reference of the power controlling MMC is set as zero when the DC voltage controlling MMC regulates the DC voltage to its rated value. Then, the power will be ramped up by the power controlling MMC and the power reversal process of the MMC link is accomplished. The power reversal process of the MMC link is summarized in Table II.

TABLE II
SEQUENCE TO REVERSE THE POWER FLOW OF THE HB-MMC LINK

Sequence	Actions
Reduce power	Power control
Block MMCs	Converter block
Disconnect MMCs from AC grids	Open $\mathrm{BRK_{AC}}$ and $\mathrm{BRK_{R}}$
Disconnect MMCs from the DC line and the neutral ground	Open S_{P1} and $\mathrm{S_{N2}}$
Discharge the DC line	Close S_{D}
Stop discharging when the DC line voltage drops to zero	Open S_{D}
Reconfigure MMC's connection with the DC line	Close $\mathrm{S_{P2}}$ and $\mathrm{S_{N1}}$
Connect the MMC to the AC grid	Close $\mathrm{BRK_{AC}}$
Bypass the start-up resistor when the DC voltage reaches valve-side AC line voltage	Close $\mathrm{BRK_{R}}$
Deblock converters	Deblock control
Control the DC voltage to the rated value	DC voltage control
Power ramp up	Power control

As for the LCC link, its power reversal process is different from the MMC link. The power will be reduced to the minimum value (e.g. 0.1 p.u.) when the power reversal order is received from the higher level control system. To reduce the unbalanced current between the two poles, the power reduction of the LCC link should be at the same reducing rate of the MMC link. The DC current controlling LCC will be blocked when its current is reduced to the minimum value. Then the firing angle of the DC voltage controlling LCC will be changed to regulate the DC voltage to zero. The DC voltage controlling LCC will be blocked when the DC voltage is reduced to zero. After that, the control modes of the two LCCs will be switched from rectifier to inverter or vice versa. Then the new DC voltage controlling LCC will be deblocked and start to regulate the DC voltage to the rated value. The power of the LCC link will be subsequently ramped up when the MMC link accomplishes its polarity reversal. It should be mentioned that the power ramp-up of both poles should be in the same rate to reduce the unbalance current in the metallic return. The power reversal process of the LCC link is summarized in Table III.

TABLE III
SEQUENCE TO REVERSE THE POWER FLOW OF THE LCC LINK

Sequence	Actions
Reduce power	Current control
Block the current controlling LCC	Converter block
Control the DC voltage to zero	Firing angle control
Block the DC voltage controlling LCC	Block control
Change LCCs' control modes	Switch control systems
Deblock DC voltage controlling LCC	Deblock control
Control the DC voltage to the rated value	Firing angle control
Power ramp up	Current control

B. Mixed LCC and FB-MMC Links

Thanks to the configuration of its SMs, FB-MMC is able to regulate its DC terminal voltage from 1 p.u. to -1 p.u. Therefore, the additional DC side switches and discharging resistor for HB-MMC based links are not needed in FB-MMC based links. Based on the modulation principle of MMCs [7], the DC voltage of an FB-MMC is determined by:

$$V_{\mathrm{dc}} = \sum_{i=1}^{N} (S_{\mathrm{p}i} V_{\mathrm{cap}}) + \sum_{i=1}^{N} (S_{\mathrm{n}i} V_{\mathrm{cap}}) \tag{1}$$

where $S_{\mathrm{p}i}$ and $S_{\mathrm{n}i}$ are the switching functions of the SMs in the upper and lower arms, and V_{cap} is the voltage of the SM capacitors. By changing the output of the switching functions, the output voltage of an FB-SM can be V_{cap}, 0 and $-V_{\mathrm{cap}}$. In order to achieve a stable online power reversal, the following modulation strategy [7] with changing the number of inserted SMs to regulate the DC voltage has been employed. The number of inserted SMs in the upper and lower arms is determined by:

$$\begin{cases} N_{\mathrm{up}} = \dfrac{0.5V_{\mathrm{dcref}} - V_{\mathrm{acref}}}{V_{\mathrm{crated}}} \\ N_{\mathrm{down}} = \dfrac{0.5V_{\mathrm{dcref}} + V_{\mathrm{acref}}}{V_{\mathrm{crated}}} \end{cases} \tag{2}$$

where N_{up} and N_{down} are the inserted SM number for the upper and lower arms, V_{dcref} is the DC voltage reference, V_{acref} is the AC modulation voltage, V_{crated} is the rated voltage of the SM capacitors. Then the DC voltage V_{dc} of the FB-MMC is:

$$\begin{aligned} V_{\mathrm{dc}} &= (N_{\mathrm{up}} + N_{\mathrm{down}}) V_{\mathrm{cap}} \\ &= \left(\frac{0.5V_{\mathrm{dcref}} - V_{\mathrm{acref}}}{V_{\mathrm{crated}}} + \frac{0.5V_{\mathrm{dcref}} + V_{\mathrm{acref}}}{V_{\mathrm{crated}}} \right) V_{\mathrm{cap}} \\ &= \left(\frac{V_{\mathrm{dcref}}}{V_{\mathrm{crated}}} \right) V_{\mathrm{cap}} \end{aligned} \tag{3}$$

It can be seen from (3) that the V_{dc} can be controlled by regulating V_{dcref}. During this process, only the number of inserted SMs is changed. The voltages of SM capacitors will nearly remain constant. The DC voltage controller is shown in Fig. 3. The DC voltage reference will be ramped down once the power reversal order is received.

Take the system shown in Fig. 1 as an example. Assume that the MMCs are FB-MMCs. The power reversal process of the LCC link is the same as the sequence given in Table III. The FB-MMC is controlled to coordinate with the LCC link. First, the power in the FB-MMC link is reduced to zero. Then, the DC polarity reversal control of the FB-MMC is triggered.

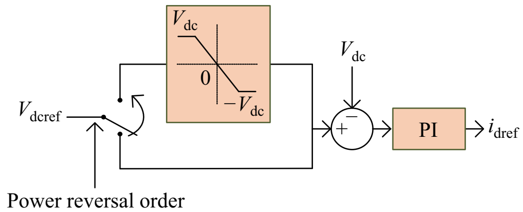

Fig. 3. DC voltage controller.

The DC voltage will be regulated from 1 p.u. to −1 p.u. The transmission power in the two links will be ramped up when the LCC link has been restarted. The sequence of the power reversal process of the FB-MMC link is summarized in Table IV.

TABLE IV
SEQUENCE TO REVERSE THE POWER FLOW OF THE FB-MMC LINK

Sequence	Actions
Reduce power	Power control
Reverse DC polarity	DC voltage control
Power ramp up	Power control

Compared to the HB-MMC, the FB-MMC scheme can be faster as no switches are used. However, it should be mentioned that the power losses and economic costs of the FB-MMC are larger than the HB-MMC, even though the FB-MMC can achieve better performance.

III. HYBRID HVDC LINKS WITH MIXED TERMINALS

The above studies discuss the power reversal strategies of bipolar hybrid HVDC links with mixed LCC and MMC poles. Due to the inherent characteristics of HB- and FB-MMCs, the power reversal strategies of hybrid LCC/HB-MMC and LCC/FB-MMC links with mixed terminals will be different. Therefore, the power reversal process of links with one LCC terminal and one MMC terminal (as shown in Fig. 4) needs to be investigated as well.

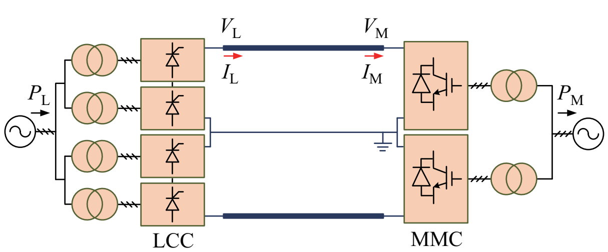

Fig. 4. A hybrid HVDC with mixed LCC and MMC terminals.

In this section, power reversal control strategies for two types of hybrid LCC/MMC links will be studied. It should be mentioned that, in this section, the LCC operates as the rectifier and regulates the DC current and the MMC operates as the inverter and regulates the DC voltage.

A. Mixed LCC and HB-MMC Terminals

As the HB-MMC cannot regulate its DC voltage to a value lower than its valve-side AC line voltage, additional DC switches in the DC side are needed to change the DC polarity of the MMC or the LCC in the link shown in Fig. 4. The setup shown in Fig. 2 and the approach proposed in [7] provide an option to change the polarity of the HB-MMC. However, this approach needs to disconnect the MMC from the AC grid and discharge the DC line. It takes extra time to restart the MMC link by re-connecting the MMC to the DC line and to re-charge the DC line. Moreover, this method involves the additional DC line discharging switch and resistor which increase the capital cost. Instead, it may be better to change the LCC's polarity. Fig. 5 shows the arrangement of the high-speed DC switches for changing the DC polarity of the LCC.

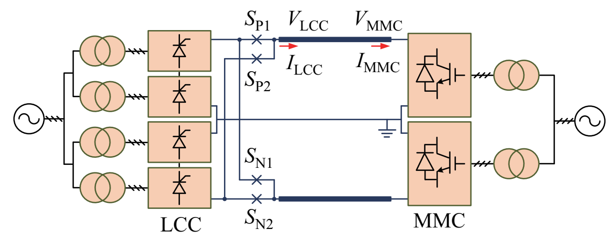

Fig. 5. The setup for changing LCC's DC polarity.

Initially, the DC switches S_{P1} and S_{N2} are closed and S_{P2} and S_{N1} are opened. The current of the LCC needs to be reduced to the minimum value when the power reversal order is received from the higher level control system. Then the LCC needs to be blocked. After that, the DC switches S_{P1} and S_{N2} will be opened under a zero current condition. Then the DC switches S_{P2} and S_{N1} will be closed. Subsequently, the LCC will be deblocked and the power will be ramped up. It should be mentioned that the control mode of the LCC does not need to be switched as its DC polarity has been reversed. The HB-MMC keeps controlling the DC voltage during the whole power reversal process. The sequence of the power reversal process of the whole system is summarized in Table V.

TABLE V
SEQUENCE TO REVERSE THE POWER FLOW

Sequence	Actions
Reduce power	Power control
Block the LCC	Converter block
Disconnect LCC from DC line	Open S_{P1} and S_{N2}
Connect LCC to DC line	Close S_{P2} and S_{N1}
Deblock the LCC	Converter de-block
Power ramp up	Power control

B. Mixed LCC and FB-MMC Terminals

Section II(B) has presented the control strategy of the FB-MMC to reverse its DC polarity online. The control strategy can also be employed in the system shown in Fig. 4, if the MMCs are FB-MMCs. Before reversing the DC voltage, the LCC will reduce the DC current to the minimum value. Then the FB-MMC will start to regulate the DC voltage to reverse the DC polarity. During the polarity reversal period, the LCC keeps regulating the DC current at the minimum value. The power will then be ramped up once the DC voltage is reversed to −1 p.u. No converter is blocked during the power reversal process. The sequence of the power reversal process of the whole system is summarized in Table VI.

TABLE VI
SEQUENCE TO REVERSE THE POWER FLOW

Sequence	Actions
LCC reduces power	Power control
FB-MMC reverses polarity	DC voltage control
LCC ramps up power	Power control

IV. HYBRID LCC/MMC MULTI-TERMINAL DC GRIDS

The above studies focus on the power reversal of point-to-point HVDC links. The power reversal for hybrid LCC/MMC MTDC grids is investigated in this section.

As an MMC can control bi-directional power flow without changing its DC voltage polarity, the difficulty of power reversal in a hybrid LCC/MMC MTDC grid relies on how to reverse the LCCs' power flow without affecting the rest of the grid. In an MTDC grid, there will be multiple converters. It may not be reasonable to change the DC polarity of the whole system aiming to reverse the power flow of a single LCC. Therefore, the possible solution is to change the DC polarity of the target LCC with the help of its DC side switches. In this case, other converters will be affected with minimum impact.

Take the 4-terminal hybrid LCC/MMC MTDC grid shown in Fig. 6 as an example. The power reversal of the MMCs can be easily done by their power control. The power reversal of LCCs can be carried out through the proposed method in Section III(A). The high-speed DC switches shown in Fig. 5 are installed in the DC terminal of each LCC. The current of the LCC will be reduced to the minimum value if a power reversal order is received from the higher level control system. The DC switches will operate to change the polarity of the LCC once it is blocked. Then the LCC will be de-blocked and the power will be ramped up. To avoid overload of the DC lines and the converters, communication among the converter stations is needed to coordinate the power-sharing within the whole system.

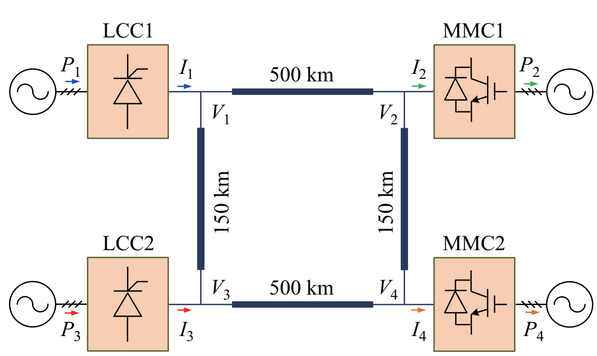

Fig. 6. A 4-terminal hybrid LCC/MMC grid.

It should be mentioned that the proposed power reversal strategies can be fully applied in both overhead line (OHL) and cable based HVDC systems. The control strategies and sequences are the same. The difference is that the speed of the power reversal in a cable based system might be slower because there might be more energy stored in a cable than in an OHL [23].

V. CASE STUDIES

The proposed control strategies for different topologies are verified in simulation models established in PSCAD/EMTDC. The LCC models are taken from the CIGRE first benchmark HVDC model [24]. The MMC control system is shown in Fig. 7. The parameters of the MMC are given in Table VII. The capacity of every LCC and MMC is equal. The parameters of the 500 kV OHL is taken from [25] and its configurations and dimensions are shown in the Appendix. In this study, a 100 ms is assumed to emulate the operating time of the AC side breakers and a 20 ms is assumed to emulate the operating time of the DC side switches.

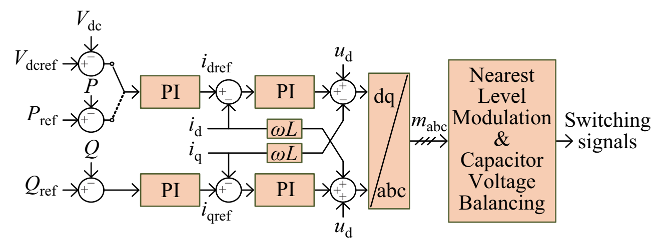

Fig. 7. MMC control system.

TABLE VII
PARAMETERS OF THE MMC

Parameters	Values
MMC capacity (single-pole) (MW)	1000
Transformer capacity (single-pole) (MVA)	1050
Rated DC voltage (kV)	500
Rated AC voltage (kV)	230
AC grid frequency (Hz)	50
MMC transformer ratio (kV/kV)	250/230
Transformer leakage reactance (p.u.)	0.18
Number of SMs in each arm	10
DC terminal inductor (H)	0.1
SM capacitance (mF)	2.5
Arm inductance L (H)	0.025
Arm resistance R (Ω)	0.1
AC system equivalent resistance R_S (Ω)	1.0375
AC system equivalent reactor L_S (H)	0.0165
AC side start-up resistor (Ω)	100
Length of the OHL (km)	500

A. Mixed LCC and HB-MMC Links

In this case, the configuration and the measurements of the test system are shown in Fig. 1. The HB-MMC link is the positive pole and the LCC link is the negative pole. The strategy proposed in Section II(A) is employed. A 2500 Ω resistor is used as the DC discharging resistor.

The time sequences of the two poles are given in Table VIII. Fig. 8 illustrates the dynamic responses of the two poles during the power reversal process. It can be seen that the power flow reversal process can be accomplished within 1.4 s. There is no severe transient overcurrent and overvoltage during the power reversal process. The negative current overshoot in the MMC link at $t = 2.85$ s is the DC line charging current caused by closing the HB-MMC's grid side breaker $\mathrm{BRK_{AC}}$. The current

TABLE VIII
TIME SEQUENCE OF THE POWER REVERSAL OF CASE A

HB-MMC Link		LCC Link	
Time	Actions	Time	Actions
$t_0 = 2.2$ s	Reduce power	$t_0 = 2.2$ s	Reduce power
$t_1 = 2.5$ s	Block MMCs	$t_1 = 2.5$ s	Block LCC 1; LCC 2 starts to reduce DC voltage
$t_2 = 2.6$ s	Open BRK_{AC} and BRK_R	$t_2 = 2.8$ s	Block LCC 2
$t_3 = 2.65$ s	Open S_{P1}, S_{N2} and S_{GND}	$t_3 = 2.9$ s	Switch LCCs' control modes
$t_4 = 2.7$ s	Close S_D	$t_4 = 3.05$ s	Deblock LCCs and ramp up power
$t_5 = 2.73$ s	Open S_D		
$t_6 = 2.75$ s	Close S_{P2}, S_{N1} and S_{GND}		
$t_7 = 2.85$ s	Close BRK_{AC}		
$t_8 = 2.90$ s	Close BRK_R		
$t_9 = 2.95$ s	Deblock MMCs; MMC 2 starts to regulate the DC voltage		
$t_{10} = 3.05$ s	Ramp up power		

in the metallic return is shown in Fig. 8 (c). It can be seen that during normal operations, there is only a minor unbalanced current which can be accurately reduced by the cooperation of the two links. The polarity reversal causes unbalanced currents in the metallic return, however, it only lasts for a limited period of time.

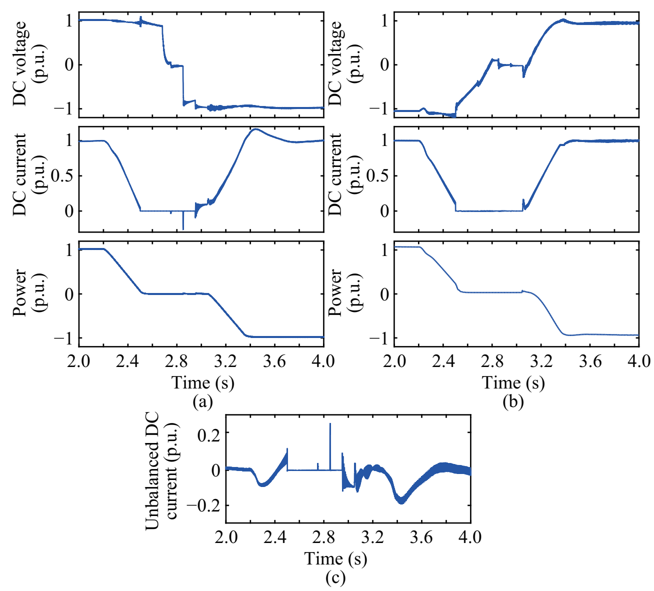

Fig. 8. Dynamic responses during the power reversal process. (a) The HB-MMC link; (b) The LCC link; (c) Current in the metallic return.

Moreover, to avoid voltage disturbances during the polarity reversal, it is important to select a high resistance value for the discharging resistor. However, this may not allow a very fast polarity reversal during emergency power control as it may take a long time to energize the DC line, especially for HVDC cables.

B. Mixed LCC and FB-MMC Links

In this case, the MMC link in Fig. 1 is assumed as an FB-MMC link. All parameters are the same as the case in Section V(A). The time sequences of the two poles are given in Table IX. Fig. 9 illustrates the dynamic responses of the test system. It can be seen that the FB-MMC link and LCC link coordinate smoothly and the power reversal is achieved within 1.25 s. The DC voltage of the FB-MMC link is reversed smoothly by the DC voltage control within 0.3 s. The slope of the voltage ramp down can be changed according to system requirements.

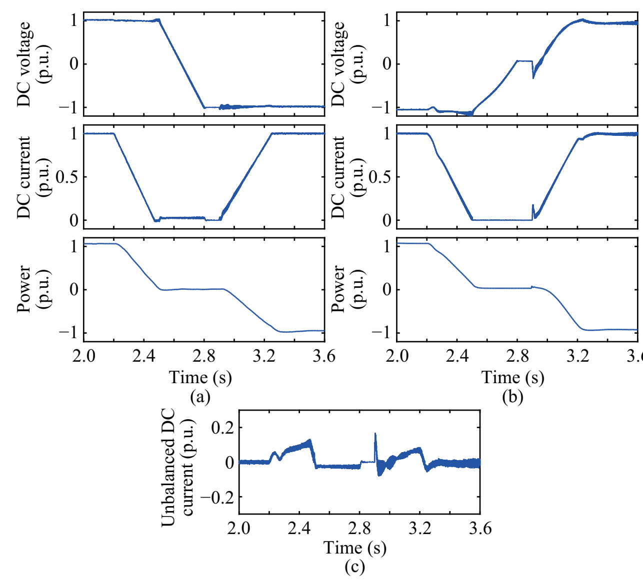

Fig. 9. Dynamic responses during the power reversal process. (a) The FB-MMC link; (b) The LCC link; (c) Current in the metallic return.

C. Mixed LCC and HB-MMC Terminals

In this case, the MMCs shown in Fig. 5 are assumed as

TABLE IX
TIME SEQUENCE OF POWER REVERSAL OF CASE B

FB-MMC Link		LCC Link	
Time	Actions	Time	Actions
$t_0 = 2.2$ s	Reduce power	$t_0 = 2.2$ s	Reduce power
$t_1 = 2.5$ s	MMC 2 reverses DC voltage	$t_1 = 2.5$ s	Block LCC 1; LCC 2 starts to reduce DC voltage
$t_2 = 2.9$ s	Ramp up power	$t_2 = 2.8$ s	Block LCC 2
		$t_3 = 2.85$ s	Switch LCCs' control modes
		$t_4 = 2.9$ s	Ramp up power

HB-MMCs. All parameters are the same as the case in Section V(A). As the positive and negative poles are symmetrical, only the positive pole is measured and is shown in Fig. 5. The time sequence of the power reversal process is given in Table X. Fig. 10 illustrates the dynamic responses of the test system. It can be seen that the power reversal is accomplished smoothly within 0.8 s. There is no transient overcurrent and overvoltage during the power reversal process.

TABLE X
TIME SEQUENCE OF POWER REVERSAL OF CASE C

Time	Actions
$t_0 = 2.2$ s	LCC reduces power
$t_1 = 2.5$ s	Block LCC
$t_2 = 2.55$ s	Open S_{P1} and S_{N2}
$t_3 = 2.6$ s	Close S_{P2} and S_{N1}
$t_4 = 2.7$ s	Deblock LCC and ramp up power

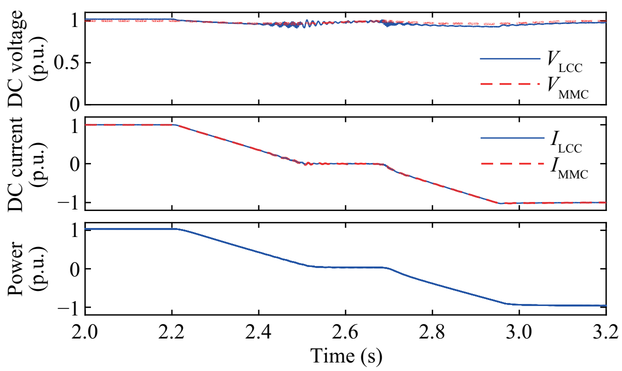

Fig. 10. Dynamic responses during the power reversal process.

D. Mixed LCC and FB-MMC Terminals

In this case, the MMC shown in Fig. 5 is assumed as an FB-MMC. All parameters are the same as the case in Section V(A). The time sequence of the power reversal process is given in Table XI. Fig. 11 illustrates the dynamic responses of the test system. It shows that the power reversal is completed within 0.9 s. There is no transient overcurrent and overvoltage during the power reversal process. It should be mentioned that the converters during the reversal process remains operating. No converter blocking is needed.

TABLE XI
TIME SEQUENCE OF POWER REVERSAL OF CASE D

Time	Actions
$t_0 = 2.2$ s	LCC reduces power
$t_1 = 2.5$ s	FB-MMC reverses DC voltage
$t_2 = 2.8$ s	LCC ramps up power

E. Hybrid LCC/MMC Multi-terminal DC Grids

The system shown in Fig. 6 is tested in this case. The two LCCs are power sending ends and the two MMCs are power receiving ends. The MMC 1 controls the DC voltage while other converters control the power. The power, current and voltage measurements are shown in Fig. 6. In the test, the LCC 1 and MMC 2 reverse their power flow consequently.

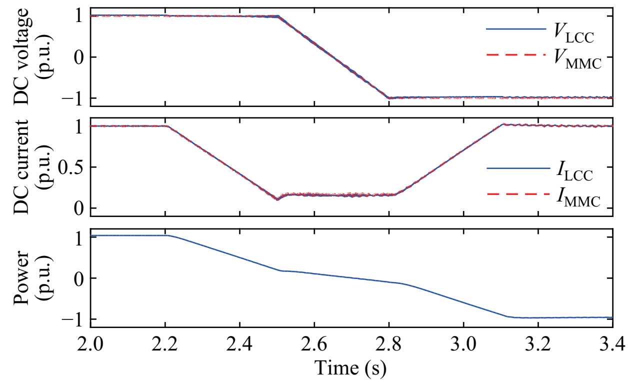

Fig. 11. Dynamic responses during the power reversal process.

The strategy proposed in Section IV is employed. The time sequence of the power reversal process is given in Table XII. The dynamic responses of the system are illustrated in Fig. 12.

TABLE XII
TIME SEQUENCE OF POWER REVERSAL OF CASE E

Time	Actions
$t_0 = 2.2$ s	LCC 1 reduces power to zero
$t_1 = 2.7$ s	Block LCC 1
$t_2 = 2.9$ s	Complete polarity changing of LCC 1
$t_3 = 3$ s	Deblock LCC1and ramp up power to 1 p.u
$t_4 = 4.25$ s	Reverse MMC 2 s power from 1 p.u. to -1 p.u.

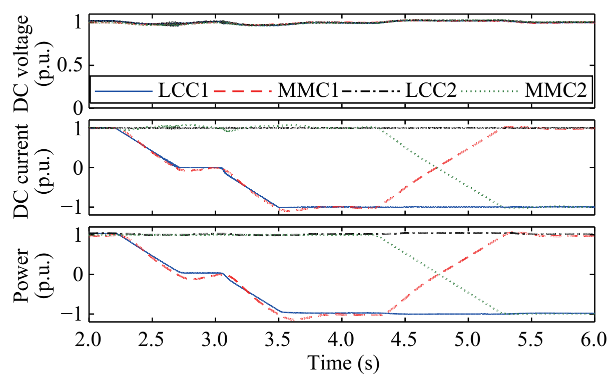

Fig. 12. Dynamic responses of the hybrid LCC/MMC grid.

The dimensions and parameters of the OHL used in this paper are shown in Fig. 12. It should be mentioned that the metallic return circuit is modeled as a resistor based on the metallic return line JNRLH60/G1A-400/35 which is applied in the ± 500 kV Zhangbei 4-terminal HVDC grid. The resistance is 0.07516 Ω/km. The datasheet can be found in [26].

It can be seen that the power reversal of the LCC 1 and MMC 2 can be completed quickly without inducing large disturbances in the whole system. As the MMC 1 operates in the DC voltage control mode, it is the "slack bus" of the system. Although MMC 1 can compensate for the power flow changing of other converters, communication among the converter stations is still needed to avoid overload of the converters and the DC lines.

It should be mentioned that the power reversal speed in real applications can be much longer (sometimes up to 100 MW per minute [5]) and the AC system strength (short-circuit ratio) can be weaker than that in the case studies conducted in this paper. It is because not only the system topologies but also other system operating conditions and requirements, such as the AC system strength, load changing and emergency power control, may impact the power reversal process. The results presented in this section prove the effectiveness of the proposed methods instead of proving which system topology and method is "faster" or "more stable." The AC system strength and power reversal speed and methods (e.g. on-line or off-line) should be considered in the design stage of HVDC systems to meet the needs of system operation.

VI. Conclusion

In this paper, the power reversal control strategies of different types of hybrid LCC/MMC HVDC systems were proposed and verified in simulations conducted in PSCAD. It can be concluded that the FB-MMC has more flexibility than HB-MMC in the power reversal of hybrid LCC/MMC systems. Additional DC side switches and discharging resistors are needed to reverse the DC voltage polarity of HB-MMCs to cooperate with the LCC link in a system with one pole of HB-MMC and the other pole of LCC. The FB-MMC can achieve a smooth online DC voltage reversal through proper modulation methods. Therefore, no additional switches are needed for hybrid LCC/FB-MMC systems. The proposed power reversal strategies can also be applied in hybrid LCC/MMC MTDC grids. It should be mentioned that the case studies in this paper just give examples of the reversal processes of the proposed strategies. The speed of the power reversal process needs to be determined by system requirements.

References

[1] G. Li, C. Y. Li, and D. Van Hertem, "HVDC technology overview," in *HVDC Grids*: *For Offshore and Supergrid of the Future*, D. Van Hertem, O. Gomis - Bellmunt, and J. Liang, Eds. Hoboken, NJ, USA: Wiley, 2016, pp. 45–76.

[2] G. Li, J. Liang, T. Joseph, T. An, J. J. Lu, M. Szechtman, B. R. Andersen, and Q. K. Zhuang, "Feasibility and reliability analysis of LCC DC grids and LCC/VSC hybrid DC grids," *IEEE Access*, vol. 7, pp. 22445–22456, Feb. 2019.

[3] G. Li, W. Liu, T. Joseph, J. Liang, and Z. M. Song, "Double-thyristor based protection for valve-side single-phase-to-ground faults in HB-MMC based bipolar HVDC systems," *IEEE Transactions on Industrial Electronics*, Aug. 2019, doi:10.1109/TIE. 2019.2931502.

[4] G. F. Tang, Z. Y. He, H. Pang, X. M. Huang, and X. P. Zhang, "Basic topology and key devices of the five-terminal DC grid," *CSEE Journal ofPower and Energy Systems*, vol. 1, no. 2, pp. 22–35, Jun. 2015.

[5] J. P. Kjærgaard, T. Pande-Rolfsen, B. Bergdahl, K. Søgaard, A. Strandem, H. O. Bjarme, and S. D. Mikkelsen, "Bipolar operation of an HVDC VSC converter with an LCC converter," in *Proceedings of the HVDC and Power Electronic Systems forOverhead Line and Insulated Cable Applications*, San Fansisco, CA, USA, 2012, pp. 1–7.

[6] G. Andersson, M. Hyttinen, and A. B. B. Sweden, "Skagerrak—the next generation," in *Proceedings of HVDC and Power Electronic Technology*, Lund, Sweden, 2015, pp. 1–9.

[7] L. J. Yu, C. Y. Guo, C. Y. Zhao, J. Z. Xu, N. An, and X. B. Hu, "Power reversal of hybrid HVDC system," inProceedings of the *11th IET International Conference on AC and DC Power Transmission*, Birmingham, 2015, pp. 1–6.

[8] G. Li, J. Liang, F. Ma, C. E. Ugalde-Loo, and H. F. Liang, "Analysis of single-phase-to-ground faults at the valve-side of HB-MMCs in HVDC systems," *IEEE Transactions on Industrial Electronics*, vol. 66, no. 3, pp. 2444–2453, Mar. 2019.

[9] G. Tang and Z. Xu, "A LCC and MMC hybrid HVDC topology with DC line fault clearance capability," *International Journal of Electrical Power & Energy Systems*, vol. 62, pp. 419–418, Nov. 2014.

[10] W. Xiang, S. Z. Yang, L. Xu, J. J. Zhang, W. X. Lin, and J. Y. Wen, "A transient voltage-based DC fault line protection scheme for MMC-based DC grid embedding DC breakers," *IEEE Transactions on Power Delivery*, vol. 34, no. 1, pp. 334–345, Feb. 2019.

[11] R. E. Torres-Olguin, M. Molinas, and T. Undeland, "Offshore wind farm grid integration by VSC technology with LCC-based HVDC transmission," *IEEE Transactions on Sustainable Energy*, vol. 3, no. 4, pp. 899–907, Oct. 2012.

[12] D. H. R. Suriyaarachchi, C. Karawita, and M. Mohaddes, "Tapping existing LCC-HVdc systems with voltage source converters," in *Proceedings of 2016 IEEE Power and Energy Society General Meeting*, Boston, MA, 2016, pp. 1–5.

[13] M. H. Nguyen, T. K. Saha, and M. Eghbal, "Hybrid multi-terminal LCC HVDC with a VSC converter: a case study of simplified South East Australian system," in *Proceedings of 2012 IEEE Power and Energy Society General Meeting*, San Diego, CA, 2012, pp. 1–8.

[14] T. An, X. X. Zhou, C. D. Han, Y. A. Wu, Z. Y. He, H. Pang, and G. F. Tang, "A DC grid benchmark model for studies of interconnection of power systems," *CSEE Journal of Power and Energy Systems*, vol. 1, no. 4, pp. 101–109, Dec. 2015.

[15] Y. T. Wang and B. H. Zhang, "A novel hybrid directional comparison pilot protection scheme for the LCC-VSC hybrid HVDC transmission lines," in *Proceedings of the13th International Conference on Development in Power System Protection 2016*, Edinburgh, 2016, pp. 1–6.

[16] C. Y. Guo, W. J. Liu, and C. Y. Zhao. "Research on the control method for voltage-current source hybrid-HVDC system," *Science China Technological Sciences*, vol. 56, no. 11, pp. 2771–2777, Nov. 2013.

[17] G. Li, J. Liang, T. Joseph, T. An, M. Szechtman, B. Andersen, and Q. K. Zhuang, "Start-up and shut-down strategies of hybrid LCC/VSC DC grids," in *Proceedings of the 2nd IEEE Conference on Energy Internet and Energy System Integration*, Beijing, China, 2018, pp. 1–5.

[18] G. Li, W. Liu, T. Joseph, J. Liang, T. An, J. J. Lu, M. Szechtman, B. Andersen, and Q. K. Zhuang, "Control strategies of full-voltage to half-voltage operation for LCC and hybrid LCC/MMC based UHVDC systems," *Energies*, vol. 12, no. 4,pp. 742, Feb. 2019.

[19] N. M. Haleem, A. D. Rajapakse, A. M. Gole, and I. T. Fernando, "Investigation of fault ride-through capability of hybrid VSC-LCC multi-terminal HVDC transmission systems," *IEEE Transactions on Power Delivery*, vol. 34, no. 1, pp. 241–250, Feb. 2019.

[20] J. Arrillaga, A. Erinmez, and D. B. Giesner, "Power-reversal control in h. v. d. c. interconnectors," *Proceedings of the Institution of Electrical Engineers*, vol. 119, no. 9, pp. 1345–1350, Sep. 1972.

[21] U. Radbrandt, "Method and arrangement to reverse the power flow of a direct current power transmission system," U.S. Patent 20100091528A1, Apr. 15, 2010.

[22] J. Xu, C. Y. Zhao, T. Li, J. Z. Xu, H. Pang, and C. Lin, "The hybrid HVDC transmission using line commutated converter and full bridge modular multilevel converter," in *Proceedings of the 2nd IET Renewable Power Generation Conference*, Beijing, 2013, pp. 1–4.

[23] H. T. Wang, J. Z. Cao, Z. Y. He, J. Yang, Z. Y. Han, and G. Chen, "Research on overvoltage for XLPE cable in a modular multilevel converter HVDC transmission system," *IEEE Transactions on Power Delivery*, vol. 31, no. 2, pp. 683–692, Apr. 2016.

[24] M. Szechtman, T. Wess, and C. V. Thio, "First benchmark model for HVDC control studies," *Electra*, vol. 135, pp. 54–67, 1991.

[25] P. Liu, R. F. Che, Y. J. Xu, and H. Zhang, "Detailed modeling and simulation of +500 kV HVDC transmission system using PSCAD/EMTDC," in *Proceedings of 2015 IEEE PES Asia-Pacific Power and Energy Engineering Conference*, Brisbane, QLD, 2015, pp. 1–3.

[26] Data sheet of JNRLH60/G1A-400/35. [Online]. Available: http://www.tacsr.com/caseshow.php?cid=38&id=71&lang=1.

Gen Li (M'18) received the B.Eng. degree in Electrical Engineering and its Automation from Northeast Electric Power University, Jilin, China, in 2011, the M.Sc. degree in Power Engineering from Nanyang Technological University, Singapore, in 2013 and the Ph.D. degree in Electrical Engineering from Cardiff University, Cardiff, U. K., in 2018.

From 2013 to 2016, he was a Marie Curie Early Stage Research Fellow funded by the European Union's MEDOW project. He has been a Visiting Researcher at China Electric Power Research Institute and Global Energy Interconnection Research Institute, Beijing, China, at Elia, Brussels, Belgium and at Toshiba International (Europe), London, U. K. He has been a Research Associate at the School of Engineering, Cardiff University since 2017. His research interests include control and protection of HVDC and MVDC technologies, power electronics, reliability modelling and evaluation of power electronics systems.

Dr. Li is a Chartered Engineering in the U. K. He is an Associate Editor of the CSEE Journal of Power and Energy Systems. His Ph.D. thesis received the First CIGRE Thesis Award in 2018.

Ting An received her B.Sc. degree from Xi'an Jiaotong University, China in 1982, her M.Sc. degree from the Graduate School of China Electric Power Research Institute (CEPRI) in 1985, and her Ph.D. degree from the University of Manchester (former UMIST), the United Kingdom in 2000, respectively.

From 1985 to 1990 she was an Electrical Engineer with CEPRI. From 1991 to 1999 she worked for GE (former ALSTOM) T&D Power Electronic Systems Limited as a Senior Engineer in the UK. Between 1999 and 2013, she was a Principal Consultant with E. ON New Build & Technology in the UK. Currently, she is a State Specially Recruited Expert, a Chief Expert and Technical Director for oversea projects at the Global Energy Interconnection Research Institute (GEIRI) of the State Grid Corporation of China (SGCC), China. She is a Charted Engineer in the UK and a fellow of the IET. She was a member of CIGRE B4/C1.65 WG and is the convener for CIGRE WG B4.72. She is a guest professor at the Institute of Electrical Engineering, Chinese Academy of Sciences and Shaanxi University of Technology respectively. Her research interests include R&D research on VSC-HVDC and HVDC Grids, power electronics, and integration of off-shorewind power via HVDC technology.

Jun Liang (M'02–SM'12)received his B.Sc. degree in Electric Power System & its Automation from Huazhong University of Science and Technology, Wuhan, China, in 1992 and his M.Sc. and Ph.D. degrees in Electric Power System & its Automation from the China Electric Power Research Institute (CEPRI), Beijing, in 1995 and 1998, respectively.

From 1998 to 2001, he was a Senior Engineer with CEPRI. From 2001 to 2005, he was a Research Associate with Imperial College London, U. K.. From 2005 to 2007, he was with the University of Glamorgan as a Senior Lecturer. He is currently a Professor in Power Electronics with the School of Engineering, Cardiff University, Cardiff, U. K. He is a Fellow of the Institution of Engineering and Technology (IET). He is the Chair of IEEE UK and the Ireland Power Electronics Chapter. He is an Editorial Board Member of CSEE JPES. He is the Coordinator and Scientist-in-Charge of two European Commission Marie-Curie Action ITN/ETN projects: MEDOW (€3.9 M) and InnoDC (€3.9 M). His research interests include HVDC, MVDC, FACTS, power system stability control, power electronics, and renewable power generation.

Wei Liu (M'18) received his B.Sc. and M.Sc. degrees from Zhejiang University, Hangzhou, China, in 2012 and 2015, respectively.

From 2015 to 2017, he was a research engineer with Rongxin Huiko Electric Technologsy Co., Ltd. China. From 2017 to 2018, he was a research assistant at Aalborg University, Denmark. Since April 2018, he has been a Marie Curie Early Stage Research Fellow in the InnoDC project and working towards his Ph.D. degree at Cardiff University, UK. His research interests include HVDC technologies, and renewable power generation.

Tibin Joseph (S'13–M'16) received his B.Tech. and M.Tech. degrees in Electrical Engineering from Mahatma Gandhi University, Kerala, India, in 2008 and 2011 respectively. From 2012 to 2013 he worked as a Lecturer at Mahatma Gandhi University, Kerala, India. He obtained the Ph.D. degree in Electrical and Electronic Engineering from Cardiff University, Wales, U. K. in 2018. He was a Marie Curie Early Stage Researcher between 2013 and 2016 at Cardiff University. He has been a visiting researcher at CEPRI in Beijing, China, and at the National Grid, Warwick, U. K. Since 2017 he has been working as a Research Associate at Cardiff University. His research interests include DC transmission and distribution systems, asset management, power system stability and control, subsynchronous oscillations, and renewable energy integration.

Jingjing Lu received her B.S. and Ph.D. from the Department of Electrical Engineering, North China Electric Power University (NCEPU), Beijing, China, in 2010 and 2015, respectively. She was a visiting scholar at the University of Connecticut, Storrs, CT, USA, from December 2013 to October 2014. She is presently working at the Global Energy Interconnection Research Institute. Her fields of interest are DC grid planning and high-power electronic technology in power systems.

Marcio Szechtman (M'72–F'96–LF'18) received his B.Sc. and the M.Sc. degrees from University of Sao Paulo- Brazil, in 1971 and 1976, respectively.

From 1976 to 1997, he was a Senior Researcher at CEPEL, the Brazilian Power Research Institute. From 1997 to 2016, he worked as an Independent Consultant in the areas of HVDC and FACTS. Since January 2017, he has been the Director General for CEPEL. Between 2002 and 2008, he acted as Chairman of the CIGRE Study Committee B4. In 2014, he received the CIGRE Medal. In 2017, he was elected as Chairman of the Technical Council of CIGRE. In 2018, he became Life Fellow for IEEE/PES. His research interests include HVDC, FACTS, power system stability control, power electronics, and environmental planning.

Bjarne R Andersen (SM'02–F'14) is the Director and Owner of Andersen Power Electronic Solutions Limited, which was established in 2003. Before becoming an independent consultant, he worked for 36 years for what is now GE Grid, where his final role was as Director of Engineering. He was involved with the development of the first chain link STATCOM and the relocatable SVCs concept. He has extensive experience in all stages of LCC and VSC HVDC projects. As a consultant, he has worked on several international HVDC projects, including the Caprivi Link, the first commercial VSC HVDC project to use an HVDC overhead line, and a VSC HVDC project for multi-terminal operation permitting multi-vendor access. He was the Chairman of Cigre SC 14 from 2008 to 2014 and initiated several working groups in the area of HVDC Grids. He is an Honorary member of Cigre, and was the 2012 recipient of the prestigious IEEE PES Uno Lamm Award.

Yuanliang Lan received his B.S. and M.S. degrees in electrical engineering from Northeast China Electrical Power Institute, Jilin province, China in 1994 and 1997 respectively, and his Ph.D. degree at China Electrical Power Research Institute (CEPRI) in Beijing, China in 2006. Currently he is the chief engineer at Innovative Energy Technology Group of GEIRI-EU and His research interests include Renewable energy integration, FACTs and HVDC, Intelligent power electronics *etc*.